Magnetic properties of hydrogenated amorphous Fe–Si–B fiber

A. Mitra, A. K. Bhattamishra, and I. Chattoraj

Citation: Journal of Applied Physics **73**, 2443 (1993); doi: 10.1063/1.353101
View online: http://dx.doi.org/10.1063/1.353101
View Table of Contents: http://scitation.aip.org/content/aip/journal/jap/73/5?ver=pdfcov
Published by the AIP Publishing

Magnetic properties of hydrogenated amorphous Fe–Si–B fiber

A. Mitra,[a] A. K. Bhattamishra,[b] and I. Chattoraj[b]
National Metallurgical Laboratory, Jamshedpur-831007, India

(Received 13 July 1992; accepted for publication 19 October 1992)

Magnetic properties of a hydrogenated amorphous Fe–Si–B fiber have been studied. Hydrogen was charged electrochemically. Saturation magnetization and the switching characteristics of the fiber have been investigated for different charging conditions. Saturation magnetization is found to decrease with the increase of charging time and charging current density. Variation of switching characteristics with the charging conditions is rather complex. Magnetic properties have also been studied during degassing of hydrogen. Hydrogen inside the specimen induces tensile stress due to volume expansion and at the same time modifies Fe–Fe exchange interaction. The magnetic behavior due to hydrogenation and during degassing have been explained by considering the dual role of hydrogen inside the fiber.

I. INTRODUCTION

Hydrogen absorption in metals and alloys plays an important role in modifying the electronic structure, which consequently changes the magnetic and mechanical properties of the materials.[1] The modification of the magnetic properties may be extended to a level of vanishing transition metal moments in some metal hydrides, whereas the appearance of ferromagnetism may also be observed in some alloys.[2] This drastic change in magnetic properties due to hydrogenation makes the magnetic study a suitable tool to probe the structure of hydrogenated materials.[1] Hydrogen can be incorporated, both into the crystalline and amorphous alloys. Unlike crystalline materials, where metal hydrides can be formed with more or less definite stoichiometric ratios, hydrogen produces an interstitial solid solution in amorphous alloys. So far, all the studies on amorphous alloys have been restricted to thin films or melt-spun ribbons.[3–5] To the best of our knowledge there has been no study on the hydrogenation of fiber-shaped amorphous materials. The internal stress distribution in amorphous fibers are found to be different from that of the ribbon-shaped materials, as a result of which their as-received state demonstrates different magnetic properties.[6] The most striking difference is in their flux reversal characteristic. Unlike usual ferromagnetic material, magnetostrictive amorphous fiber shows a large and stable Barkhausen jump when the applied field crosses a critical value.

In this work the effects of electrochemical hydrogen charging on the magnetic properties of amorphous $Fe_{77.5}Si_{7.5}B_{15}$ have been studied. The magnetic properties during degassing of hydrogen have also been investigated in the present work.

II. EXPERIMENT

Amorphous fibers having nominal composition $Fe_{77.5}Si_{7.5}B_{15}$ obtained from Unitika, Japan were used for the present study. A 10 cm length and 125-μm-diam fiber was taken for each experiment. Hydrogen was charged by the standard electrolytic procedure.[7] The samples formed the cathode of a cell with platinum anode and 1 N H_2SO_4 as the electrolyte. As it is very difficult to measure the hydrogen content in the fiber whose radial dimension is very small, hydrogen estimation was made in terms of charging current density (I_{ch}) and charging time (t_{ch}). Magnetic measurements were made using a hysteresisgraph (MH-3020, Walker Scientific Instruments, USA) at a frequency of 1 Hz. Measurements were made in an open flux configuration without any demagnetization correction. The maximum applied field was 35 Oe. Saturation magnetization was determined by an approach to the saturation method.[8]

III. RESULTS

The low field magnetic hysteresis loops of amorphous fibers for three different charging current densities (I_{ch}), maintaining the charging time (t_{ch}) constant at two hours, are shown in Fig. 1. It shows a wide variation in the switching field (H^*) and total change of magnetization (M^*) at the switching fields. The high field behavior is also shown in Fig. 2 for three different current densities (0, 5, and 40 mA/cm^2). Each sample was charged for two hours. To obtain a much detailed picture of the magnetization behavior after hydrogen charging, the saturation magnetization (M_s), the switching field (H^*), and the total change of magnetization (M^*) at the switching field are plotted in Figs. 3 and 4 with different charging conditions. All the magnetic parameters are normalized with the corresponding as-received value. The results, when the charging time was varied up to 8 h, keeping the charging current density constant at 25 mA/cm^2 are shown in Fig. 3, whereas the results with the variation of charging current, keeping the charging time constant at 2 h, are shown in Fig. 4. Figure 3 shows that the normalized value of total change in magnetization, m^* ($=M^*_{(\text{charged})}/M^*_{(\text{as-received})}$), increases with the charging time and reaches a maximum value for the specimen, subjected to two hours of charging. It remains almost constant at this constant value up to 4 h of charging and then starts decreasing. The normalized

[a]MTP Division.
[b]CRP Division.

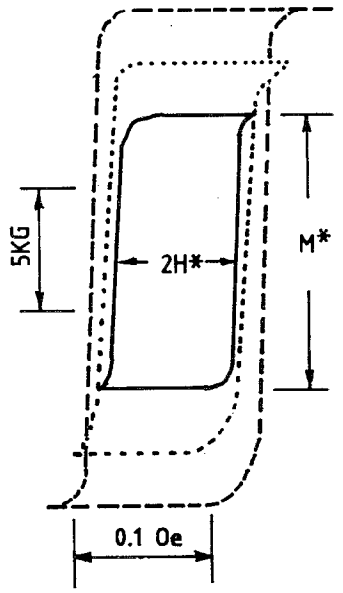

FIG. 1. Low field hysteresis loops for three different current densities: $I_{ch}=0$ (—), 5 mA/cm^2 (---), 40 mA/cm^2 (···) for charging time (t_{ch})=2 h.

switching field, h^* ($=H^*_{(\text{charged})}/H^*_{(\text{as-received})}$), increases with the charging time and attains a constant value within 1 h of charging. Here h^* remains constant up to 4 h of charging and then suddenly increases rapidly. The normalized value of saturation magnetization, m_s ($=M_s^{(\text{charged})}/M_s^{(\text{as-received})}$), decreases with the charging time and tends to level off for higher charging times. On varying the charging current density (Fig. 4), a monotonic increase in m^* and h^* is observed, which saturated for higher charging current densities. Here m_s decreases with the charging current densities and tends toward a constant value.

Time-dependent magnetic properties of the fiber after hydrogen charging was also investigated in the present study. The fiber was precharged with a current density of 25 mA/cm^2 for 24 h. Magnetic measurements were made at different times after removing the fiber from the electrolytic bath and the results are presented in Fig. 5. Here h^* increases at the beginning and then decreases below the as-received value. The initial value of m^* is more than that

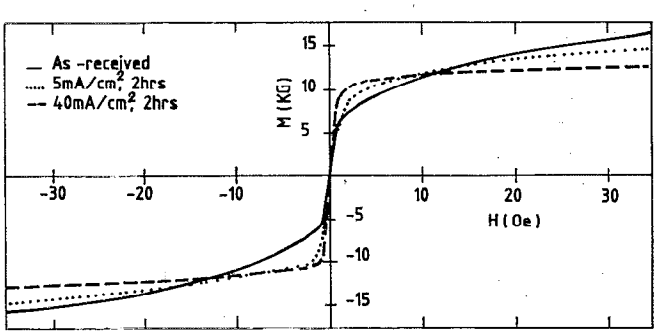

FIG. 2. High field magnetization curve for three different current densities: $I_{ch}=0$ (—), 5 mA/cm^2 (---), 40 mA/cm^2 (···) for charging time t_{ch}=2 h.

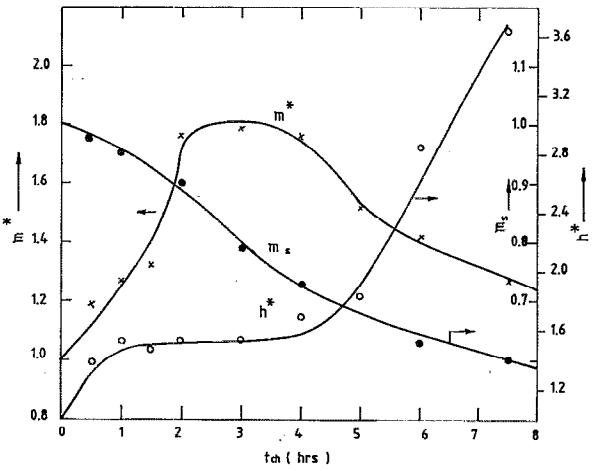

FIG. 3. Variation of normalized magnetic parameters m_s(●), $m^*(x)$, h^*(○) with charging times (t_{ch}) keeping charging current density constant (25 mA/cm^2).

of the as-received sample. It decreases below the as-received value due to degassing and shows a minimum after degassing for 5×10^3 min; m^* then increases slowly toward the as-received state. Saturation magnetization (m_s) decreases after charging and slowly increases on degassing towards its as-received state.

IV. DISCUSSION

Amorphous fibers are produced by the in-water quenching technique, where the molten metal is cooled by a rapidly rotating water stream.[9] In this method of preparation, the outer surface solidifies first and then the inner core solidifies and shrinks. Due to this differential cooling process a unique stress distribution occurs, resulting in two

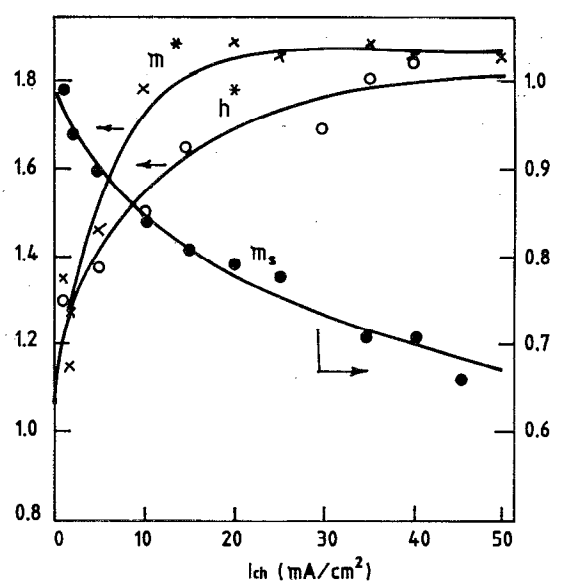

FIG. 4. Variation of normalized magnetic parameters m_s(●), $m^*(x)$, h^*(○) with charging current densities (I_{ch}) for constant charging time (2 h).

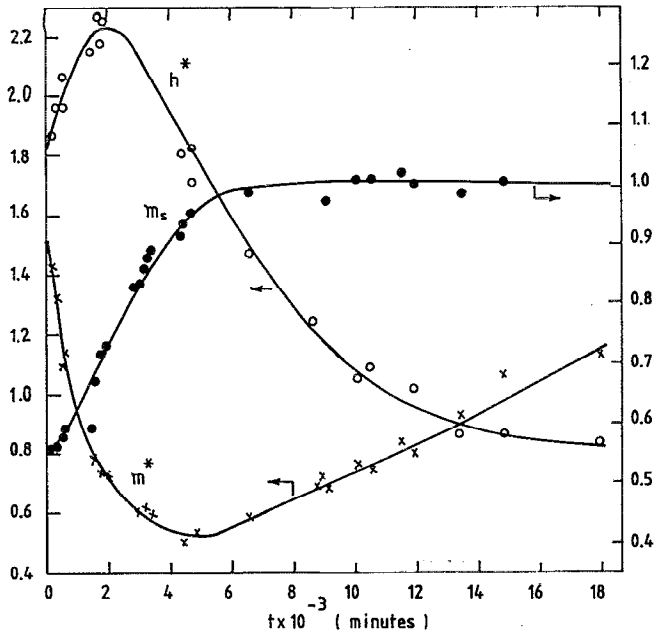

FIG. 5. Time dependence of normalized magnetic parameters (m_s,m^*,h^*) due to degassing of the precharged sample. Charging was done with 25 mA/cm^2 for 24 h.

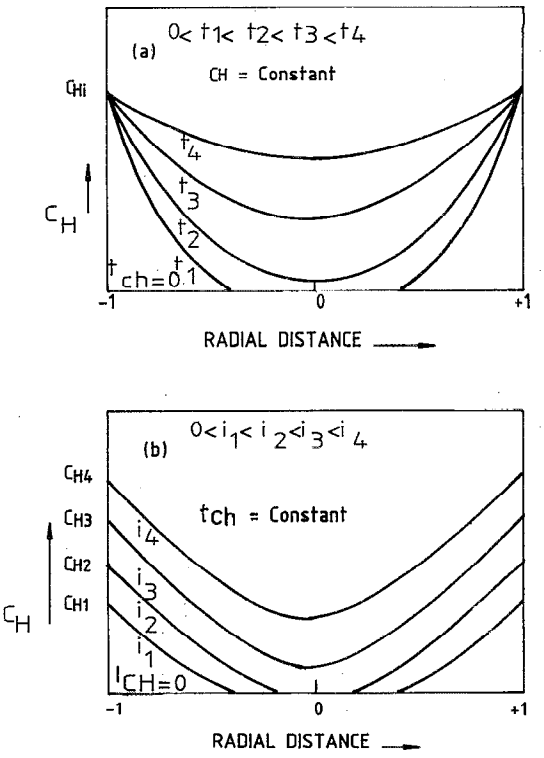

FIG. 7. Schematic representation of the hydrogen concentration profile with (a) charging times and (b) charging current densities.

distinct anisotropy regions in the magnetostrictive fiber. In the case of positive magnetostrictive fibers like $Fe_{77.5}Si_{7.5}B_{15}$, the moments of the inner core, where the stresses are tensile, are oriented along the length of the fiber, resulting in an axial anisotropy region in the core. The outer shell, where the stresses are along the radial directions, produces radial anisotropy. Besides these two anisotropy regions, a zig–zag domain pattern is observed along the periphery of the fiber.[10] Neglecting this zig–zag domain region for simplicity, the anisotropy function, $P(K)$, of the fiber can be schematically represented, as shown in Fig. 6. The maximum positive and negative values correspond to the anisotropies with the moment direction parallel and perpendicular to the fiber axis, respectively. The volume of the inner core is defined by the location of the transition region, where the anisotropy function changes from negative to the positive value, and this transition region depends on the magnetoelastic energy of the sample. The domain of the inner core is rigid and pinned by the outer shell. The magnetization thus flips from one state to another by the applied field only when the Zeeman energy exceeds the pinning energy and hence a large Barkhausen jump is observed at H^*. Therefore, H^* is directly proportional to the pinning energy and M^* is a good measure of the inner core volume.

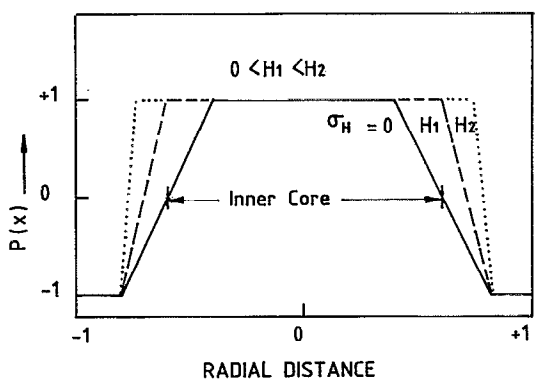

FIG. 6. Simplified model of the magnetoelastic anisotropy distribution function, $P(K)$. Positive and negative values correspond to the anisotropy axis parallel and perpendicular to the axis, respectively. Here σ_H represents induced stress due to the diffusion of hydrogen.

According to the Fick's law, hydrogen will diffuse into the matrix during electrochemical charging and the concentration profile of hydrogen in the specimen will be determined by the charging time and charging current density. Figures 7(a) and 7(b) represent schematically the hydrogen concentration (C_H) profiles at various charging times and current densities, respectively. The diffused hydrogen occupies the interstitial sites in the amorphous alloy and causes volume expansion, which is tantamount to increase in the tensile stress. With this additional tensile stress (σ_H), the anisotropy distribution will be modified, as shown schematically in Fig. 6. The initial increase of M^* with the charging time and current can be attributed to the increase of the inner core volume due to the tensile stresses exerted by hydrogen that diffuses into the specimen. The diffused hydrogen also generates extra pinning centers resulting in the increase of H^* with the charging time and current. Besides this stress effect, hydrogen also modifies the Fe–Fe exchange interaction by changing the interatomic distances. The decrease of saturation magnetization

with increasing charging time and current density can be attributed to the decrease of Fe moments due to the change of exchange interaction. For low charging times hydrogen will be confined only to the outer shell of the fiber. So at this charging time a reduction in magnetization occurs only in the outer shell of the fiber, and this reduction in moments does not affect M^*, which is related to the inner core properties. But hydrogen located in the outer shell exerts tensile stress, resulting in the increase of inner core volume, which, in turn, increases M^*. As the charging time is increased hydrogen will enter into the inner core, reducing the inner core moment. Thus, there will be competitive effects of induced tensile stress and a reduction of Fe moments during hydrogenation. Induced tensile stresses will try to enhance the inner core volume resulting in an increase in M^*, while the reduction of Fe moments in the inner core tends to decrease the value of M^*. These two competitive process result in a maximum in M^* with charging time. Besides this tensile effect, hydrogen also acts as a mobile pinning point. These two effects increases the Zeeman energy, and hence H^* increases with the increase of charging time and current density. The variation of magnetic property can be expected until the hydrogen concentration attains the value of surface hydrogen concentration in the specimen. The effect of increasing charging current density (Fig. 4) is a shift of surface hydrogen concentration toward higher values. This increased hydrogen concentration at the surface induces an extra tensile force and enhances M^* and H^*. The increased hydrogen concentration also reduces the Fe moment, which, in turn, reduces saturation magnetization. However, the concentration can increase until the maximum solubility of hydrogen at the surface reached. Subsequently there will be no change of magnetic parameters. The rapid increase of H^* for higher charging time is probably due to the damage of the specimen produced by hydrogen, which generates extra pinning centers.

The dual role of hydrogen is also evident when the magnetic response is studied during the degassing of a charged specimen (Fig. 5). The increase of saturation magnetization as time passes is attributed to the diffusion of hydrogen away from the specimen. This degassing operation also reduces the overall induced tensile stress on the specimen and hence M^* decreases. At later times, when hydrogen diffuses out from the inner core, the Fe moments of the inner core increases. Again, due to the competitive effect, M^* shows a minimum and tends toward its value in an as-received state with the passage of time. The initial increase in H^* is probably due to part of the hydrogen, diffusing out from the core, being trapped at some extraordinary sites generated during charging at high current densities for longer times. Such trapping would increase the total pinning energy, in spite of hydrogen degassing (i.e., a reduction of mobile pinning points). With time, the effect of these high-energy pinning centers is offset by the significant reduction of hydrogen by degassing and H^* decreases toward its value in the as-received state.

V. CONCLUSION

The two distinct anisotropy regions (radial and longitudinal) in amorphous fibers are generated due to the unique distribution of internal stresses produced during preparation. The large Barkhausen jump is observed when the Zeeman energy is sufficient to flip the moments of the longitudinal anisotropy region from one state to other. The magnetic properties are found to change significantly when the fiber is charged by hydrogen. Saturation magnetization decreases, whereas M^* and H^* increases with the charging current density and ultimately saturates. Similar behavior is also observed for M_s when the charging time is varied. After the saturation, a rapid increase in H^* is observed when the charging time is varied. Here M^* shows a maximum with the charging time. The variation of magnetic properties can be explained by the dual role of hydrogen. Its entry into the specimen increases the tensile stress, which results in an increase of the longitudinal anisotropy region in positive magnetostrictive materials like $Fe_{77.5}Si_{7.5}B_{15}$ and at the same time decreases the Fe moments by modifying the exchange interaction. This dual role of hydrogen also explains the degassing behavior. The unusual behavior of H^* at higher charging times is probably due to the damage produced in the specimen by charging, which act as extra pinning centers.

ACKNOWLEDGMENT

The authors are grateful to the Director, National Metallurgical Laboratory, for providing the necessary facilities to carry out the work.

[1] A. T. Pedziwiter, E. B. Boltich, W. E. Wallace, and R. S. Craig, in *Electronic Structure and Properties of Hydrogen in Metals*, edited by P. Jena and C. B. Satterthwaite, published in cooperation with the NATO Scientific Affairs Division (Plenum, New York, 1983), p. 367.
[2] W. E. Wallace, in *Topic in Applied Physics*, edited by G. Alefeld and J. Volki (Springer-Verlag, Berlin, 1978), Vol. 28, Chap. 7.
[3] J. M. D. Coey, D. H. Ryan, D. Gignout, A. Lienard, and J. P. Rebouillat, J. Appl. Phys. **53**, 7804 (1982).
[4] B. S. Berry and W. C. Pritchet, Phys. Rev B **24**, 2299 (1981).
[5] N. Moser and H. Kronmuller, Phys. Lett. A **93**, 2101 (1982).
[6] A. Mitra and M. Vazquez, J. Magn. Magn. Mat. **87**, 130 (1990).
[7] W. Chambron, F. Lancon, and A. Chamberod, Scr. Met. **18**, 29 (1984).
[8] S. Chikazumi, in *Physics of Magnetism* (Wiley, New York, 1964), p. 274.
[9] T. Masumoto, I. Ohnaka, A. Inoue, and M. Hagiwara, Scr. Met. **15**, 293 (1981).
[10] Y. Makino, J. L. Costa, V. Madurga, and K. V. Rao, IEEE Trans. Magn. **MAG-25**, 3620 (1989).